Fish and Shellfish Immunology 99 (2020) 473–482

Contents lists available at ScienceDirect

Fish and Shellfish Immunology

journal homepage: www.elsevier.com/locate/fsi

Full length article

Hypoosmotic stress induced tissue-specific immune responses of yellowfin seabream (*Acanthopagrus latus*) revealed by transcriptomic analysis

Genmei Lin[a,1], Min Zheng[a,1], Dong Gao[a], Shizhu Li[a], Wenyu Fang[a], Jing Huang[a], Jingui Xie[a], Jingxiong Liu[a], Yijing Liu[a], Zhaohong Li[a], Jianguo Lu[a,b,*]

[a] School of Marine Sciences, Sun Yat-sen University, Zhuhai, 519082, China
[b] Southern Marine Science and Engineering Guangdong Laboratory (Zhuhai), Zhuhai, 519080, China

ARTICLE INFO

Keywords:
Yellowfin seabream
Hypoosmotic stress
Osmoregulation
Immune responses
RNA-Seq analysis

ABSTRACT

Salinity is a limiting factor for many marine organisms, including fishes. The shift in the ambient salinity can cause osmotic stress and arouse immune responses in fish. In this study, yellowfin seabream (*Acanthopagrus latus*), a euryhaline marine teleost, was used to investigate immune responses of different tissues (gill, liver, and muscle) under hypoosmotic stress. Comparative transcriptomic and physiological analyses of three tissues were conducted after fish exposed to the fresh water (FW, salinity = 0 ppt), low-saline water (LW, salinity = 3 ppt), and brackish water (BW, salinity = 6 ppt) for 8 days. The results showed that hypoosmotic stress dramatically altered the gene expression of three tissues in yellowfin seabream; The investigation of differentially expressed genes (DEGs) related to osmoregulation and immune response indicated that T cell-mediate immunity pathways were essential to tackle such stress. In terms of tissues, gill was found to be the most sensitive tissue under hypoosmotic stress by enhancing of Na^+K^+-ATPase activity and preventing the loss of Na^+ and K^+; Liver, on the other hand, was under the most sever oxidative stress indicated by the fluctuation of SOD, CAT activities and the MDA content; In contrast, muscle had the least osmoregulation and immune related response. We also identified several potential candidate genes, which may serve as gene indicators to identify the stressor. Overall, this study provides preliminary mechanistic insights into hypoosmotic stress adaption of aquatic organism.

1. Introduction

Salinity is a major abiotic factor in the environment for all aquatic organisms [1]. A change in the salinity of habitat water can lead to osmotic stress and influence hormonal levels, metabolic and energetic parameters and osmoregulation or immune response, *etc.* in fish [2–4]. One of the most important regulatory systems to tackle such stress is immune system. Stress induced by salinity changes can agitate the generation of reactive oxygen species (ROS) that may compromise the efficacy of immune system and cause oxidative stress [5]. Marine fish can also recognize and respond to salinity variation by altering the expression of genes specifically required for osmoregulation [1].

To identify such abiotic stress, researchers reported a series of innovative analytical approaches, including flow cytometry, automatic blood cell analysis, micro-Raman spectroscopy and ^{1}H NMR and immunohistochemical assays to assess the health status of aquaculture species under the stress condition such as diseases, environmental changes and presence of pollutants [6–10]. For example, analyzing the whole-blood samples of fish by flow cytometry could tell that the increasing water salinity induced erythropoiesis in teleost fish species [11]. If the underpinning genes and related mechanisms are concerned, transcriptomics is the most researched omics technology for such purpose.

Most of studies related to osmotic stress in fish have been focus on the hyperosmotic stress [12–16], in which they stated that acute or chronic salinity changes could inhibit the expression of some immune-related genes and arouse both cellular and humoral immune activities. Nonetheless, hypoosmotic stress could also modulate the immune homeostasis of fish [17].

As euryhalines, the fish must be able to cope with salt depletion and water gain when it is in fresh water. It was reported that when gilthead seabream (*Sparus aurata*) was acclimated to water with the low salinity of 6 ppt, it exhibited lower peroxidase and alternative complement activity in plasma compared to those acclimated to water with higher salinity (12 ppt and 38 ppt) [13]. Another study stated that broad-nosed pipefish (*Syngnathus typhle*) at low salinity were unable to mount

* Corresponding author. School of Marine Sciences, Sun Yat-sen University, Zhuhai, 519082, China.
E-mail address: lujianguo@mail.sysu.edu.cn (J. Lu).
[1] Authors contributed equally to this work.

https://doi.org/10.1016/j.fsi.2020.02.028
Received 9 October 2019; Received in revised form 12 February 2020; Accepted 14 February 2020
Available online 16 February 2020
1050-4648/

specific immune response components upon bacterial infection [12]. However, studies evaluating fish acclimation to hypoosmotic environment and the underline mechanism of such stressors on the immune capacity remain largely unexplored.

Yellowfin seabream, *Acanthopagrus latus* (Houttuyn), is an economically and ecologically important marine fish which is broadly distributed throughout the Indo-West Pacific area including southern Japan, southeastern China, Taiwan, Persian Gulf, and Australia [18–21]. Owing to its excellent quality and good taste, it has been successfully farmed in Southeast Asia since the 1980s [22]. The salinity level for offshore culture in south China has been reported within the range of 4–10 ppt for this species [22–24]. Inevitably, yellowfin seabream could encounter hypoosmotic stress when moving from coastal waters to offshore brackish water culture environment. Earlier studies related to salinity adaption of yellowfin seabream had been focused on their morphological [25] and physiological [26] responses. However, the underline adaption molecular mechanism especially for hypoosmotic stress is unclear.

In this study, we employed the next-generation sequencing (NGS) technology to sequence and *de novo* assembled the gill, liver, and muscle transcriptome of yellowfin seabream in the brackish water (BW, salinity = 6 ppt), the low-saline water (LW, salinity = 3 ppt), and the fresh water (FW, salinity = 0 ppt) environments. The aim of this study is to identify immune system related transcriptomic differences associated with FW- and LW-acclimated tissues within a single species along with the related metabolic pathways. To our best knowledge, this is the first NGS study that had provided a differential transcriptome-wide perspective among tissues of a euryhaline fish acclimated to FW and LW. Also, these candidate immune related genes may be used as molecular biomarkers to diagnose stress in fish, improve stress tolerance and reduce diseases of fish in the activities of aquaculture and fisheries stock enhancement.

2. Material and methods

2.1. Fish maintenance and salinity challenge experiment

All protocols were carried out in accordance with the Ethic Committee on the Care and Use of Laboratory Animals of Sun Yat-sen University, Guangzhou, China.

Yellowfin seabream with average body length of 11.2 ± 0.9 cm and body weight of 36.93 ± 10.57 g were obtained from a local fish farm (Zhuhai, China) at a salinity of 6.06 ± 0.47 ppt, Then the fish were transferred to our lab and kept in the tank filled with brackish water (BW) in the salinity of 5.98 ± 0.09 ppt for two weeks for adaption to the new condition before exposing them to other salinity variations. Fish were maintained at 26.5 ± 0.5 °C under a 14h/10h light-dark photoperiod with automated water circulation and gentle aeration. During this period, fish were fed with red worm twice daily. No mortality was recorded during the entire acclimation period.

Three salinity including ~6, 3 and 0 ppt were used in this study in triplicate. Fish were fasted 24h before salinity challenge. After acclimation, fish were suddenly exposed to fresh water (FW, the salinity was adjusted to 0.10 ± 0.03 ppt) or low-saline water (LW, the salinity was adjusted to 2.94 ± 0.40 ppt) respectively (n = 12 per tank). One group remained in the brackish water (n = 12) as a control. Each tank was filled with 54L water under the culture conditions mentioned above. After 8 days [27], the survival rates of yellowfin seabream were 100%, 100% and 58% in BW, LW, and FW group respectively.

Three fishes per tank were anesthetized with tricaine methane sulfonate (MS 222, 200 mg/L) and sampled immediately. The tissues (gill, liver, and muscle) were collected and stored at −80 °C till use.

2.2. Physiological parameter analyses

Gill, liver, and muscle tissues from the same individual from each group were collected for physiological analyses. Tissues were homogenized in 1.0 mL deionized water for Na^+ concentration, K^+ concentration, and Na^+K^+-ATPase (NKA) activity measurements or normal saline for superoxide dismutase (SOD) activity, catalase (CAT) activity, and the malonic dialdehyde (MDA) contents measurements on ice. After centrifugation, the supernatant was transferred to a new tube and used for physiological analyses. Commercially kits were used to test Na^+ concentration, K^+ concentration, NKA activity, SOD activity, CAT activity and the MDA contents of three tissues following the manufacturer's protocol (Nanjing Jiancheng Bioengineering Institute, China). The total protein content was analyzed following the iodine-starch colorimetric method.

2.3. RNA extraction, library construction, and transcriptome sequencing

Total RNA was extracted using TRIzol Reagent (Invitrogen, USA) following manufacturer's instructions. Briefly, the tissues were homogenized using bead-beating homogenizer (TOMOS, China) and resuspended in 1 mL TRIzol solution. The mixture was shaken, incubated at room temperature for 5 min and centrifuged at 4 °C. Then the supernatant was removed to a new tube and mixed with 200 μL chloroform. The mixture was vortexed, incubated at room temperature for 5 min, and centrifuged for 10 min at what 10,000 × *g* at 4 °C. The supernatant was mixed with 500 μL isopropanol and stored at −20 °C for 1 h and then kept at room temperature for 10 min. The RNA was precipitated and washed twice with 1 mL 70% RNase-free ethanol, then air dried, and resuspended in 100 μL DEPC (diethyl pyrocarbonate)-treated water.

The concentration and purity of extracted RNA was checked using a NanoDrop 2000 Spectrophotometer (Thermo Fisher Scientific, USA). The quality of RNA was checked through electrophoresis in 1% agarose gel to confirm there was no degradation and genomic DNA contamination. The integrity of RNA was assessed using the RNA Nano 6000 Assay Kit of the Agilent Bioanalyzer 2100 system (Agilent Technologies, USA).

RNA with RIN value above 8.0 was used for library construction. The library was generated using Truseq™ RNA Sample Prep Kit (Illumina, USA) following manufacturer's instructions. Briefly, mRNA was purified from the total using oligo (dT)-attached magnetic beads, which was then fragmented using fragmentation buffer. The first-strand cDNA was synthesized using random hexamer primers and reverse transcriptase. The second-strand cDNA was synthesized subsequently using RNase H and DNA polymerase I. The double stranded cDNA was polished blunt ended with end repair mix. After dA addition at the 3′ ends of cDNA fragments, adaptors with hairpin loop structure were added. The cDNA was enriched and amplified through PCR. The PCR product was purified, and its quality was assessed on Bioanalyzer 2100 system (Agilent, USA). The libraries were pair ends sequenced on Illumina Hiseq™ platform (Shanghai Majorbio Bio-pharm Technology Co., Ltd, China).

2.4. Bioinformatic analyses

Raw reads were first trimmed and quality-filtered using Trimmomatic v0.38 [28]. GC content, Q20, Q30, and sequence duplication level were calculated through FastQC v0.11.8. Transcriptome was assembled using Trinity v2.8.4 [29] with default parameters. The Trinity assembly was optimized using CD-HIT v4.6.8 [30] and TransRate v1.0.3 [31] and then evaluated using BUSCO v3 [32]. Databases including NR (NCBI non-redundant protein sequences), GO (Gene ontology), KEGG (Kyoto encyclopedia of genes and genomes ortholog database), KOG (Clusters of eukaryotic orthologous groups of proteins), Pfam (Protein family), and Swiss-Prot (A manually annotated and reviewed protein sequence database) were applied to gene annotation.

Transcript abundance was quantified and normalized into Transcripts Per Million reads (TPM) with RSEM v1.2.15 [33].

Differential expression of genes between libraries was analyzed using the DESeq2 R package [34]. The threshold for differentially expressed genes (DEGs) was p-adjust value < 0.005 and $\log_2|\text{foldchange}| > 1$. For functional annotation and classification, the DEGs were enriched into GO terms and KEGG pathways using Goatools [35] and KOBAS [36], with p-adjust value < 0.05 considered statistically significant.

The six physiological parameters (including Na^+, K^+ concentration, NKA activity SOD, CAT activity, and the MDA contents) and total transcript abundance of each KEGG pathways under "immune system" category were used for correlation analysis by R using rcor.test [37] and with "qvalue" package [38] for false positives test.

2.5. qRT-PCR validation

To assess the expression level of randomly selected DEGs, extracted RNA used for transcriptome sequencing was also used to perform qRT-PCR. Briefly, total RNA was reverse transcribed into cDNA using PrimeScript™ RT reagent Kit with gDNA Eraser (TaKaRa, China). qRT-PCR was carried out on a LightCycler® 480 II System (Roche Diagnostics, Switzerland) using TBGreen® *Premix Ex Taq*™ II (TaKaRa, China). The primer sequences for the target genes are listed in SI Table S1. The cycle threshold (Ct) values of target genes were normalized to housekeeping gene *β-actin* expression level as internal control using the $2^{-\triangle\triangle Ct}$ method. All qRT-PCR experiments were performed in triplicate.

2.6. Statistical analyses

The significant differences of physiological parameters among each group were performed by one-way analysis of variance (ANOVA) with SPSS Version 21.0. Values with $p < 0.05$ were considered significant. All values are expressed as the mean ± standard deviation.

3. Results

3.1. Physiological analyses of the gills, livers and muscles

3.1.1. Na^+ concentration, K^+ concentration, and Na^+K^+-ATPase activity

The average of Na^+ and K^+ concentration in gills, livers, and muscles were measured in this study, and the values ranged from 2.40 ± 0.55 to 4.20 ± 0.50 mmol/gprot for concentration of Na^+, and 0.25 ± 0.07 to 1.08 ± 0.32 mmol/gprot for concentration of K^+ in three tissues. Gills harbored the highest Na^+ and K^+ concentration, whereas, muscles and livers had the lowest Na^+ and K^+ concentration, respectively. However, no significant differences of Na^+ and K^+ concentration were detected among three treatments in three tissues (Fig. 1A; Fig. 1B; SI Table S2).

Na^+K^+-ATPase (NKA), a kind of protease existing on the membrane of cells and organelles, plays a pivotal role in substances transportation, energy transformation, and information transmission. The activities of NKA in three tissues were further investigated. In gills, the values of NKA activity in FW group (3.52 ± 0.83 U/mgprot, p-value < 0.01) were found significantly increased compared with that in LW group (2.04 ± 0.53 U/mgprot) and BW group (2.31 ± 0.60 U/mgprot) Nonetheless, no significant differences were found for the average value of NKA activity among three treatments in livers and muscles (liver: 0.19 ± 0.03 U/mgprot; muscle: 1.00 ± 0.20 U/mgprot) (Fig. 1C).

3.1.2. SOD activity, CAT activity and the MDA contents

As shown by the results (Fig. 1D; Fig. 1E), the antioxidant capability of yellowfin seabream was significantly compromised upon FW exposure in gills, as indicated by the significant inhibition of SOD activity (71.2% of SOD activity of BW exposure group with p-value < 0.05) and reduction of CAT activity (35.8% of CAT activity of BW exposure group) in the FW group. While, in LW group, SOD and CAT activities were enhanced 1.46-fold and 1.30-fold compared with those in BW group. Furthermore, the MDA levels significantly increased in FW (1.75-fold) and LW (1.30-fold) groups compared with those in BW group (Fig. 1F).

The SOD, CAT activities, and the MDA contents in livers had more obvious responses ($p < 0.01$) than those in gills across treatments, yet with similar regulation patterns (Fig. 1D; Fig. 1E; Fig. 1F). It demonstrated the importance of liver in osmoregulation of yellowfin seabream. Whereas, in muscles, only SOD activity was significantly depressed about 40.5% and 4.4% in FW and LW group compared with those in BW group. In contrast, CAT activity and the MDA contents showed no significant changes across three groups (Fig. 1D; Fig. 1E; Fig. 1F).

3.2. Transcriptomic analyses of the gills, livers and muscles

3.2.1. Transcriptome de novo assembly and functional annotation

The results revealed that the salinity change induced dramatic alterations in global gene transcription profiles in three tissues of yellowfin seabream. It produced approximately a total of 77.69 Gbp, 70.73 Gbp, and 86.32 Gbp clean sequence data for the gill, liver, and muscle tissue samples, respectively, with an average GC percentage of 50.03%. The average of Q20 and Q30 were 97.52% and 92.74%, respectively (SI Table S3). Clean reads were assembled into 102,215 unigenes (hereafter genes). The lengths ranged from 201 bp to 26,594 bp, with an N50 length of 2089 bp and an average length of 1270 bp (SI Fig. S1).

Of these genes, 35,697 (34.92%) were annotated by referring to the currently available databases including NR, GO, KO, Swiss-Prot, Pfam, and KOG (Table 1); We utilized GO assignment programs for functional categorization of those annotated genes, and they were able to map 12,329 genes (12.06%) to GO terms. In many cases, multiple terms were assigned to the same transcript. This resulted in assignments of 7347 genes to cellular components (CC), 6364 to biological processes (BP), and 10,227 to molecular functions (MF) (SI Fig. S2). A total of 22,987 genes (22.49%) involved in 43 KEGG secondary metabolic pathways were detected in our transcriptome database (SI Fig. S3). In addition, 12,701 genes (12.43%) were divided into 24 KOG clusters (SI Fig. S4).

In order to identify transcripts conserved in the 3 tissues (gill, liver, and muscle) and those unique to each tissue under hypoosmotic stress, a comparative analysis among the yellowfin seabream transcriptomes was conducted (Fig. 2).

In gill, a total of 1347 genes (up-regulated DEGs: 518, 38.46%, down-regulated DEGs: 829, 61.54%) were identified as DEGs in FW group compared to BW group (Fig. 2A), and significantly enriched into 53 GO terms (SI Tables S4) and 33 KEGG pathways (SI Table S5). In contrast, only 10 and 17 DEGs were found up and down regulated in LW group compared to BW group respectively (Fig. 2D). A total of 27 DEGs were enriched in 7 KEGG pathways (SI Table S5). However, no GO terms were enriched in this case (SI Table S4).

In liver, compared with BW, 1116 genes were differentially expressed in FW. Among them, 782 genes (70.07%) were up-regulated, whereas, 334 genes (29.93%) were down-regulated (Fig. 2B). These DEGs were further enriched into 13 KEGG pathways, while no significantly enriched GO terms were found (SI Table S6; SI Table S7). For comparison, a total of 525 DEGs (up-regulated DEGs: 171, 32.57% and down-regulated DEGs: 354, 67.43%) were found in LW group compared with those in BW group (Fig. 2E), which were identified enriched into 19 GO terms and 4 KEGG pathways (SI Table S6; SI Table S7).

In muscle, a total of 1584 DEGs (728, 45.96% up-regulated and 856, 54.04% down-regulated) were found in FW group compared with those in BW group (Fig. 1C), which were further significantly enriched in 7 GO terms and 8 KEGG pathways (SI Table S8; SI Table S9). In LW group, on the other hand, fewer DEGs were found compared with BW. Namely, only 33 (19, 57.58% up-regulated and 14, 42.42% down-regulated) DEGs were identified (Fig. 1F) and enriched in 2 KEGG pathways but not in any GO terms (SI Table S8; SI Table S9).

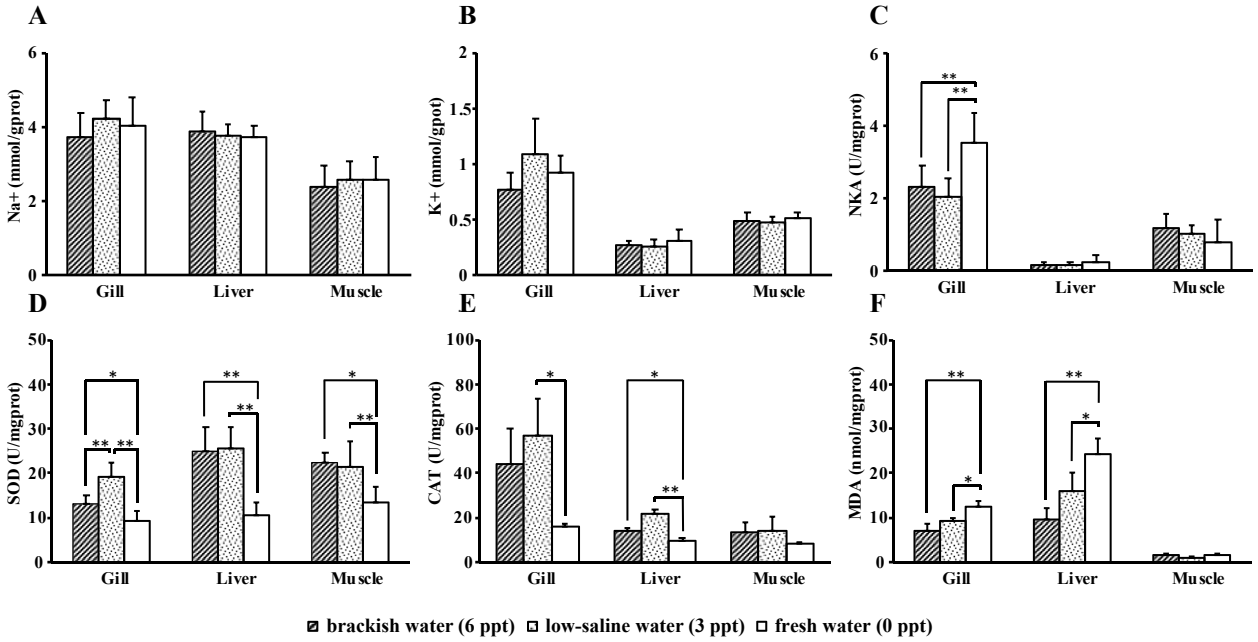

Fig. 1. Physiological parameters of gills, livers and muscles in yellowfin seabream exposed to fresh, low-saline and brackish water for 8 days. (A) Na^+ concentrations; (B) K^+ concentrations; (C) Na^+K^+-ATPase activities; (D) SOD activities; (E) CAT activities; and (F) The MDA contents.
$^*p < 0.05$ and $^{**}p < 0.01$ indicate significant difference between each group.

Table 1
Summary of annotated unigenes of yellowfin seabream.

Database	Number of annotated unigenes	Percentage of annotated unigenes (%)
NR	33,673	32.94
Swiss-Prot	28,554	27.94
Pfam	25,335	24.79
KOG	12,701	12.43
GO	12,329	12.06
KEGG	22,987	22.49
Annotated in at least one database	35,697	34.92
Total	102,215	100.00

Note: NR, NCBI non-redundant protein sequences; Swiss-Prot, a manually annotated and reviewed protein sequence database; Pfam, Protein family; KOG, Clusters of eukaryotic orthologous groups of proteins; GO, Gene ontology; KEGG, Kyoto encyclopedia of genes and genomes ortholog database.

3.2.2. Analysis of DEGs for osmoregulation in three tissues of yellowfin seabream

Specifically, DEGs related to osmoregulation in three tissues of yellowfin seabream were further identified in three tissues and mainly classified into three GO terms, including regulation of ion transmembrane transport (GO:0034,765) (Fig. 3A), integral component of membrane (GO:0016,021) (Fig. 3B), and ATP binding (GO:0005524) (Fig. 3C). Description of selected DEGs was listed in SI Table S11.

In teleost fish, gill is one of the major tissues to maintain osmotic balance by coordinated water and ion transport [39,40]. As shown in our data, gill harbored more osmoregulation related DEGs than liver and muscle (DEGs: 23 in gill, 21 in liver, and 17 in muscle) (Fig. 3). DEGs including *kcnj15* (ATP-sensitive inward rectifier potassium channel 15) and *atp* (Na^+K^+-ATPase alpha subunit) showed significantly up-regulation, while *clic4* (chloride intracellular channel protein 4) and *ncp4* (sodium channel protein type 4 subunit alpha-like) were significantly down-regulated in FW group compared with BW group (Fig. 3). Strikingly, significant up-regulation of *hsp70* (heat shock protein 70) multigene family were identified in gill (about 17.89 and 22.25 folds) in FW group compared with that in BW group (Fig. 3).

Although liver and muscle are not the main osmo-regulatory tissues, several classical ion transporters were also found in our DEG list. To our surprise, the expression of *slc22a16* (solute carrier family 22 member 16) was found about 92-fold up-regulated in the liver of FW group compared with that in BW group (Fig. 3B). Another DEG worthwhile to mention is *cret1l* (sodium- and chloride-dependent creatine transporter 1-like) which performed similarly to *slc22a16* and showed approximately 61-fold over-expression under hypoosmotic stress (FW group) (Fig. 3B). In addition, *hsp70* genes were found significantly over-expressed in liver (35.67 and 47.21-fold) in FW group compared with those in BW group as well (Fig. 3C). In muscle, multiple genes were found significantly down-regulated by approximately 6- to 9-fold, such as *ncp4*, *kcna7* (potassium voltage-gated channel subfamily A member 7-like), *aqp7* (aquaporin-7), and *grp78* (78 kDa glucose-regulated protein) in FW compared with those in BW group. Whereas, *slc22a16, cret1l*, *ntat* (large neutral amino acids transporter small subunit 2-like isoform X2), and *nslc3* (sodium-coupled neutral amino acid transporter 3), were found significantly up-regulated by about 6- to 11-fold in FW group compared with their counterparts in BW group.

It is noteworthy that the DEGs associated with osmoregulation in LW group showed the same regulation pattern but with lower fold change values compared with those identified in FW group.

3.2.3. Analysis of DEGs for immune responses in three tissues of yellowfin seabream

Furthermore, immune-related DEGs were identified based on “immune system” category in KEGG pathway database. Overall, immune related DEGs had the same regulation pattern in FW and LW groups compared with those in BW group, and more profound fold changes were found in FW group (fold change: 4.17 to 29.13) than LW group (fold change: 1.00 to 2.04) in three tissues compared with BW group, yet with only one exception, that is to say, *c8g* (complement component C8 gamma chain) strikingly overexpressed in LW (10.45-fold) rather than in FW group (1.00-fold) (Fig. 4).

A series of immune-related DEGs play crucial roles in response of hypoosmotic stress in yellowfin seabream. For example, interleukin encoding DEGs, *il12p40* (interleukin 12p40), *il17af* (interleukin 17 A/F), and *il17ra1* (interleukin 17 receptor A1) were identified down-

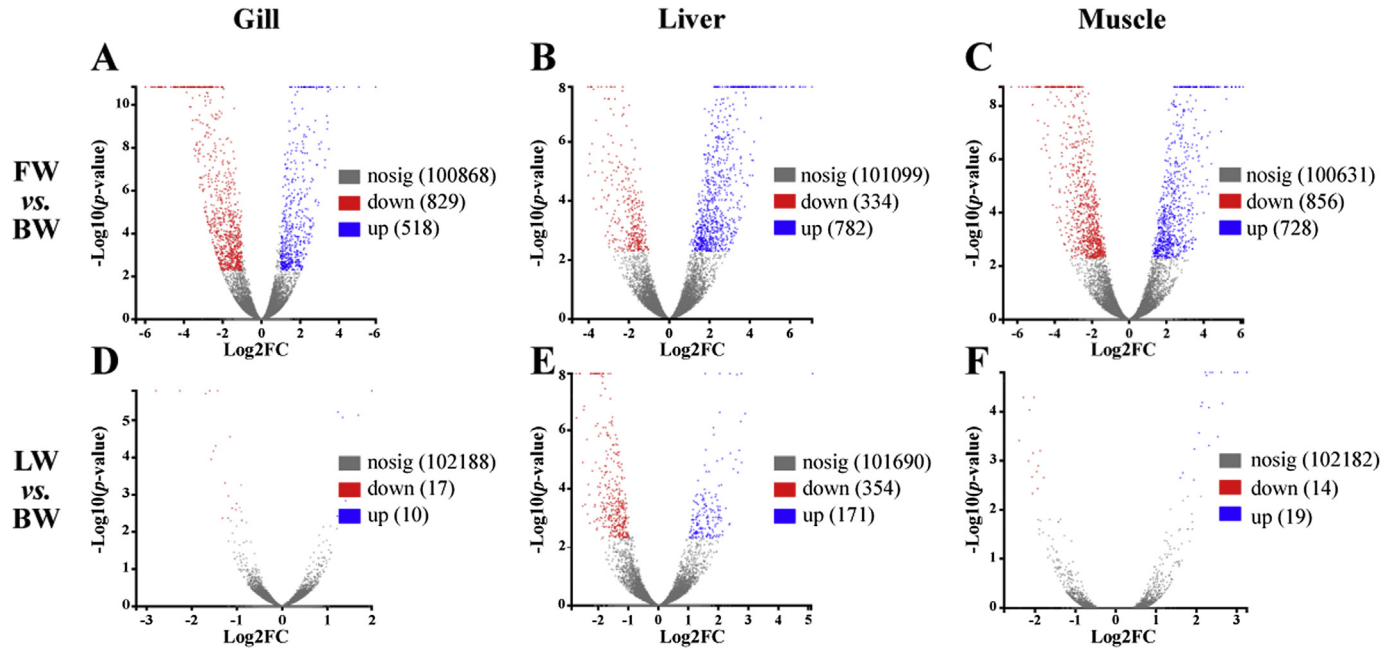

Fig. 2. Volcano plots for gill, liver and muscle gene libraries of fresh water and brackish water, or low-saline water and brackish water of yellowfin seabream by showing variance in gene expression with respect to fold change (FC) and significance (*p*-value). (A) Volcano plots for gill gene libraries of fresh water and brackish water; (B) Volcano plots for liver gene libraries of fresh water and brackish water; (C) Volcano plots for muscle gene libraries of fresh water and brackish water; (D) Volcano plots for gill gene libraries of low-saline water and brackish water; (E) Volcano plots for liver gene libraries of low-saline water and brackish water; and (F) Volcano plots for muscle gene libraries of low-saline water and brackish water. Each dot represents an individual gene: Red dots represent the down-regulated DEGs, blue dots represent the up-regulated DEGs, and grey dots represent not differentially expressed genes. (For interpretation of the references to color in this figure legend, the reader is referred to the Web version of this article.)

regulated (9.09-fold, 11.63-fold, and 4.35-fold inhibition) in gills when exposed to FW group (Fig. 4), while *il21* (interleukin-21 receptor-like) and *il20* (interleukin-20 receptor subunit alpha-like) were found over-expressed to 8.24-fold and 4.93-fold in livers under FW exposure compared with those in BW group (Fig. 4). Multiple isoforms of complement components which were significantly enriched to complement and coagulation cascades pathway were identified up-regulated in this study as well, such as *c8g* in gill and muscle, *f8l* (coagulation factor VIII-like) and *f9l* (coagulation factor IX-like) in liver (Fig. 4).

The immune-related KEGG pathway enrichment analysis was performed based on the loading stress-responsive genes to identify the significantly stress-related pathways. Overall, the majority of immune-related KEGG pathways were enriched in gill, followed by liver and then muscle. In gill, KEGG pathways including Th1 and Th2 cell differentiation (ko04658), IL-17 signaling pathway (ko04657), T cell receptor signaling pathway (ko04660), and natural killer cell mediated cytotoxicity (ko04650) were significantly enriched. Jak-STAT signaling pathway (ko04630) and NOD-like receptor signaling pathway (ko04621) were significantly enriched in liver, while B cell receptor signaling pathway (ko04662) was enriched in muscle. Furthermore, Th17 cell differentiation (ko04659) pathway was significantly enriched in both gill and liver, and antigen processing and presentation (ko04612) pathways were significantly enriched in both gill and muscle (Fig. 4). Besides, several immune related DEGs, including *btk* (tyrosine-protein kinase BTK isoform X1) and *blnk* (B-cell linker protein) in gill, *cd4* (T cell surface glycoprotein CD4) and *ccl4l* (C–C motif chemokine 4-like) in liver, as well as *gabarapl1* (gamma-aminobutyric acid receptor-associated protein-like), *samd9l* (sterile alpha motif domain-containing protein 9-like), and *c8g* in muscle were found under or over expressed with higher fold change value (absolute value $>$ 4) under salinity stress, however they didn't evoke any KEGG pathway regulation significantly (Fig. 4).

3.2.4. Validation of RNA-seq by RT-qPCR

Several members of immune-related genes in three tissues were randomly selected for further RT-qPCR validation, respectively. Fold changes represented the ratio of relative gene expression levels between FW/LW and BW treatment (Fig. 5; SI Table S10). As an internal gene, the beta-actin was included. Under the given experimental conditions, the exposure to three salinity concentration showed no effect on the internal gene (data not shown). Generally, the gene expression levels and trend of regulation (increase/decrease) detected with RNA-seq and qualification based on RT-qPCR agreed with each other.

3.3. Correlation analysis between physiological parameters and immune system related KEGG pathways

Correlation analysis demonstrated that immune system related KEGG pathways regulation correlated with osmoregulation and antioxidant activities. However, the correlation patterns varied across three tissues. In gill, six immune-related pathways showed significantly negative correlation with NKA activities with Pearson's correlation value greater than 0.992 (Table 2).

In liver, immune-related KEGG pathways in liver were positively correlated with Na^+/K^+ concentration, but negatively correlated with antioxidant activities (SI Table S12). In muscle, most immune-related KEGG pathways were negatively correlated with K^+ concentration. However, the KEGG pathways including complement and coagulation cascades (ko04610) and antigen processing and presentation (ko04612) were the exceptions. (SI Table S13).

4. Discussion

In this study, a comparative transcriptomic study along with their physiological and morphological responses of gill, liver, and muscle in yellowfin seabream exposed to different hypo salinities was conducted.

It is known that activation of NKA was considered to be related to

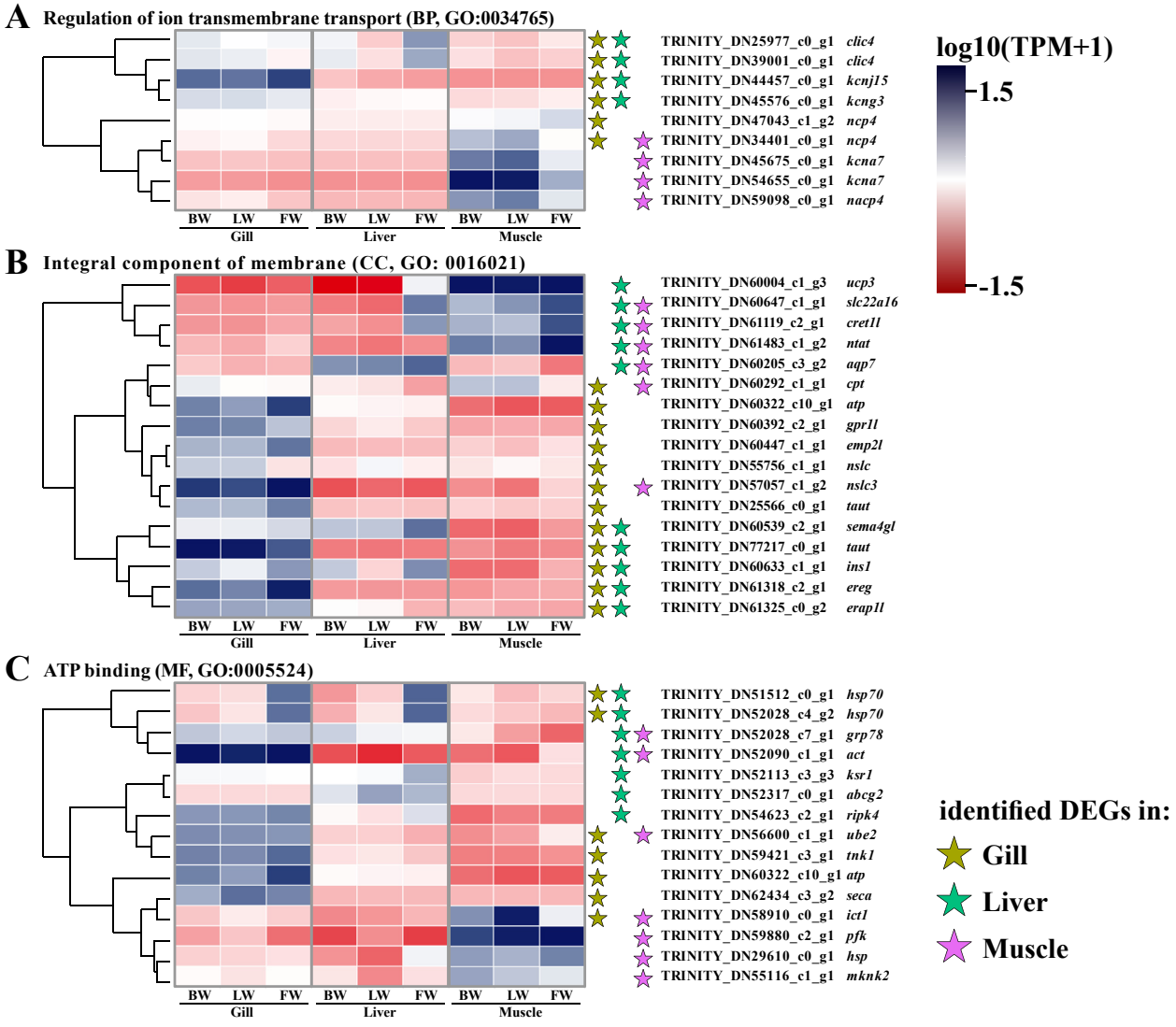

Fig. 3. Heatmap of differentially expressed genes (DEGs) annotated into osmoregulation-related GO terms in gill, liver, and muscle of yellowfin seabream exposed to fresh, low-saline and brackish water. (A) DEGs annotated into regulation of ion transmembrane transport (BP, GO:0034,765); (B) DEGs annotated into integral component of membrane (CC, GO:0016,021); and (C) DEGs annotated into ATP binding (MF, GO:0005524). BP: biological process; CC: cellular component; MF: molecular function.

Note: Data shown had the absolute fold change > 2 at $p < 0.05$. Transcript abundance was quantified and normalized into Transcripts Per Million reads (TPM) and (TPM + 1) was calculated as logs base ten.

the adaptation of cells in hypoosmotic conditions when fish are acutely exposed to a low salt environment [41]. Measurements of NKA activity, as well as Na^+ and K^+ concentration, could reflect ion transportation and homeostasis of fish body under different salinity environments. In present study, we found marked elevating NKA activity solely in gills in FW group, but no significant differences of Na^+ and K^+ concentration were detected under hypoosmotic stress. The results indicated that enhanced NKA activities may be sufficient to cope with extremely low environmental salinity by preventing the loss of Na^+ and K^+. Our finding was consistent with the result of Laiz-Carrion *et al.* [42]; who claimed the raise of NKA activity in gilthead sea bream (*Sparus auratus*) after acclimation to fresh water. However, these parameters didn't show any obvious difference in the liver and the muscle, in other words, gill is the most sensitive tissue to osmotic regulation.

Oxidative stress is one of the major stress responses when fish is exposed to various environmental stressors [43,44]. Monitoring the activity of antioxidant enzymes including SOD and CAT can imply the scavenge capacity of the antioxidant system [45]. We examined the SOD, CAT and the MDA content of three tissues in yellowfin seabream and found more obvious responses of these parameters in liver than in gills and muscles in FW group, meaning liver plays a vital role in detoxification. These findings are in agreement with Adeyemi [46]; who claimed oxidative stress were more pronounced in liver compared with that in gill and muscle.

In addition, the histological alternation was visualized to present the oxidative stress related morphological changes in tissues [44,47]. Based on our observations, more myxocytes, lamellae fusion and hyperplasia in gill were identified in FW group compared with those in BW group, which can be considered as the signs of respiration distress when fish encounters environmental stress [48,49]. Meanwhile, in FW group, more vacuolations were observed in liver, which is in line with the findings of Fanta *et al.* [50]; who had the similar observation in the liver of *Corydoras paleatus* when they were under exogenous pressure. Whereas, no obvious changes were found in muscles across three treatments (SI Fig. S5).

Lastly, transcriptome analysis was utilized to understand the immune response and underlying pathways and mechanisms of host to salinity challenges. The results demonstrated that hypoosmotic stress

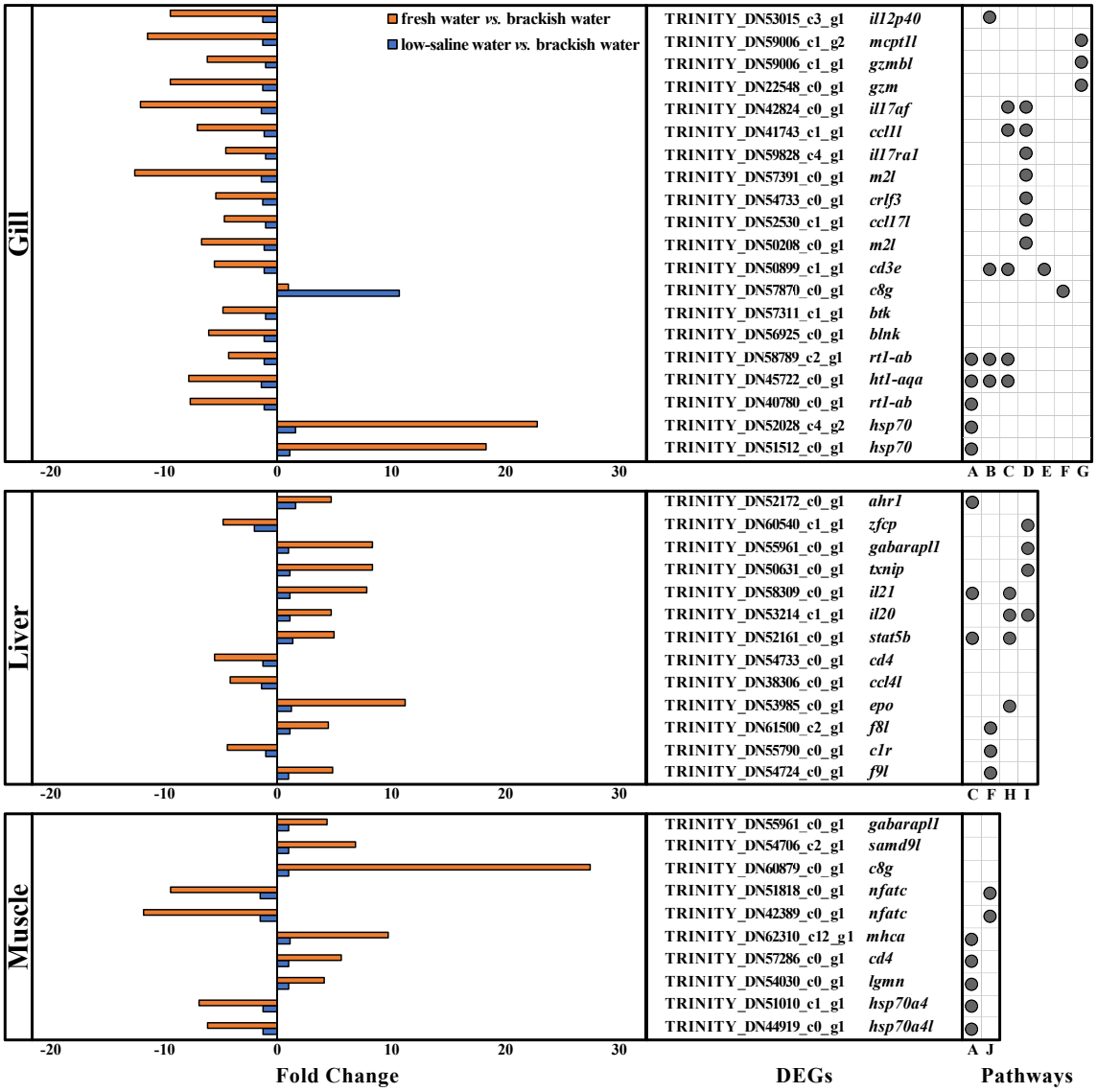

Fig. 4. Fold changes of representative immune-related differentially expressed genes (DEGs) in gill, liver, and muscle and their significantly enriched KEGG pathways of yellowfin seabream exposed to fresh, low-saline and brackish water. KGGG pathways include, A: Antigen processing and presentation; B: Th1 and Th2 cell differentiation; C: Th17 cell differentiation; D: IL-17 signaling pathway; E: T cell receptor signaling pathway; F: Complement and coagulation cascades; G: Natural killer cell mediated cytotoxicity; H: Jak-STAT signaling pathway; I: NOD-like receptor signaling pathway; and J: B cell receptor signaling pathway. Note: Data shown had the absolute fold change > 4 at $p < 0.05$.

could induce dramatic gene transcription alterations and related KEGG pathway regulations in the gill, liver, and muscle of yellowfin seabream. More osmoregulation and immune related DEGs were identified in gill compared with those in liver and muscle, further supporting that gill is one of the major tissues to maintain osmotic balance by coordinated water and ion transport. The results showed consistency with the finding in many teleost fish [39,40]. Several DEGs identified in our study might be the key genes involved in osmoregulation. For example, *hsp70* which was found up-regulated 17–22 fold in gill of FW group was also detected as a significantly regulated DEG when silver sea bream (*Sparus sarba*) was subjected to osmotic stress [51]. The other DEG *slc6a15* which was identified strikingly up-regulated (92-fold) in liver of FW group was reported as a key gene in liver of spotted sea bass for salinity adaptation [52]. A set of identified immune-related DEGs in our study such as interleukin and interleukin receptor encoding genes, were also reported as significantly regulated DEGs after salinity challenge in Asian seabass [27], spotted sea bass [52], and pipefish [12]. And the complement components could assist to link innate and adaptive immunity in fish [53–55]. The regulation pattern of DEGs associated with immune response is consistent with those aroused by osmoregulation, indicating that individuals in FW group suffered more stress and had more active immune responses than those in LW group under hypoosmotic stress. Plus, more profound fold changes of DEGs were found in FW group than those in LW group.

In addition, the significantly stress-related KEGG pathways were analyzed. The results showed majority of immune-related KEGG pathways were enriched in gill in FW group, followed by liver and then muscle. Again, it demonstrated that yellowfin seabream in fresh water suffered more stress and had more active immune responses than those in low-saline water. Overall, T cell-mediated immunity was one of the most significant responses when yellowfin seabream was subjected to hypoosmotic stress, which was consistent with the findings that T-cell activation was a key immunological consequence under osmotic stress in striped catfish based on proteomics analysis [56]. Significantly enriched immune related KEGG pathways work together to tackle the exogenous stressor. For example, in gill, antigen-presenting cells (APCs)

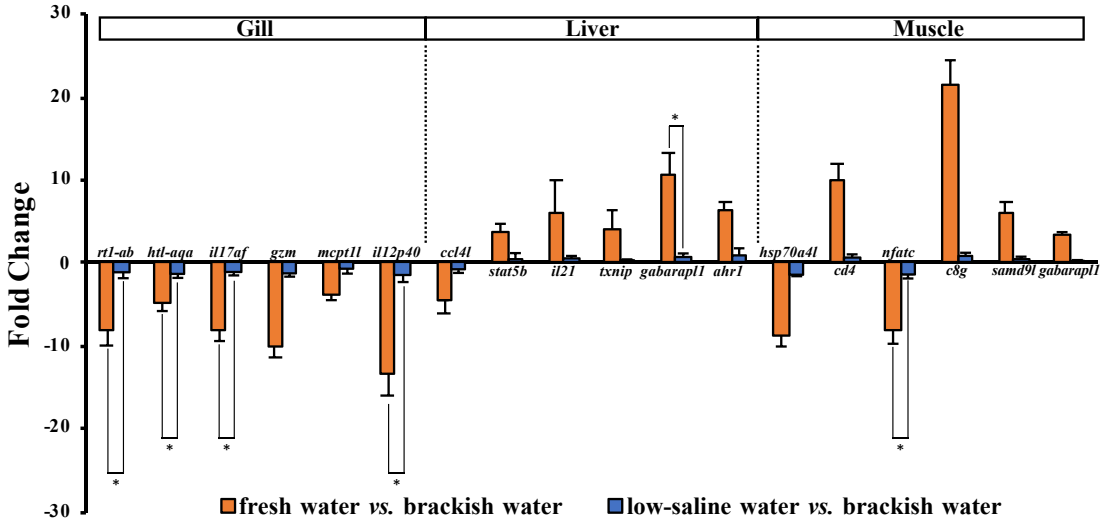

Fig. 5. Validation of gill, liver and muscle tissue transcriptome results by RT-qPCR using 18 randomly selected differentially expressed genes upon exposure to yellowfin seabream exposed to fresh, low-saline and brackish water for 8 days. The RT-qPCR fold changes are relative to brackish water samples and are normalized by changes in beta-actin values. The mean of three relative quantities of biological replicates were used in a two-tailed Student's t-test with a 95% confidence level ($p < 0.05$) to determine the gene expression significance.

could process antigens and present antigen peptide - major histocompatibility complex (MHC) -molecular complexes (ko04612) to $CD4^+$ T cells through T cell receptor signaling pathway (ko04660) [57,58], then $CD4^+$ T cells are stimulated and differentiated into distinct T helper (Th) cell subsets with different cytokines secretion. To be specific, Th1 cell supports cellular immunity, Th2 cell is functioned as B cell helper, and Th17 cells work against extracellular stressor [59]. Interleukin-17 (IL-17), a family of pro-inflammatory cytokine, could provoke both acute and chronic inflammatory responses including recruiting of inflammatory cells, producing anti-stressor peptides, and inducing secondary pro-inflammatory mediators by endothelial and epithelial tissues (ko04657). Th17 cell differentiation pathway (ko04659), cooperating with inter-regulating Th1 and Th2 cell differentiation (ko04658) could mediate defensive mechanisms to various stressor [60].

CRediT authorship contribution statement

Genmei Lin: Methodology, Validation, Formal analysis, Investigation, Data curation, Writing - original draft, Writing - review & editing, Visualization. **Min Zheng:** Formal analysis, Investigation, Data curation, Writing - review & editing. **Dong Gao:** Methodology. **Shizhu Li:** Methodology. **Wenyu Fang:** Validation. **Jing Huang:** Investigation. **Jingui Xie:** Investigation. **Jingxiong Liu:** Investigation. **Yijing Liu:** Investigation. **Zhaohong Li:** Investigation. **Jianguo Lu:** Conceptualization, Methodology, Resources, Writing - review & editing, Supervision, Project administration, Funding acquisition.

Declaration of competing interest

The authors have no competing interests to declare.

Table 2
Correlations between physiological parameters and immune-related KEGG pathways in gill.

KEGG pathway	Na^+	K^+	NKA	SOD	CAT	MDA
ko04062 Chemokine signaling pathway	−0.727	−0.847	0.695	−0.950	−0.792	0.183
ko04610 Complement and coagulation cascades	−0.087	0.109	−0.995*	0.834	0.970	−0.885
ko04611 Platelet activation	−0.306	−0.486	0.955	−0.983	−0.988*	0.634
ko04612 Antigen processing and presentation	−0.232	−0.038	−0.970	0.744	0.924	−0.943
ko04620 Toll-like receptor signaling pathway	−0.555	−0.382	−0.826	0.466	0.735	−1.000*
ko04621 NOD-like receptor signaling pathway	−0.549	−0.702	0.842	−0.997*	−0.911	0.405
ko04622 RIG-I-like receptor signaling pathway	−0.550	−0.377	−0.828	0.471	0.739	−1.000*
ko04623 Cytosolic DNA-sensing pathway	−0.673	−0.804	0.747	−0.971	−0.836	0.257
ko04624 Toll and Imd signaling pathway	0.008	0.203	−1.000*	0.882	0.989*	−0.836
ko04640 Hematopoietic cell lineage	−0.034	0.161	−0.999*	0.862	0.982	−0.859
ko04650 Natural killer cell mediated cytotoxicity	−0.586	−0.416	−0.803	0.432	0.709	−0.999*
ko04657 IL-17 signaling pathway	0.458	0.276	0.884	−0.562	−0.807	0.995*
ko04658 Th1 and Th2 cell differentiation	0.138	0.329	−0.992*	0.936	1.000*	−0.758
ko04659 Th17 cell differentiation	0.086	0.279	−0.997*	0.916	0.997*	−0.791
ko04660 T cell receptor signaling pathway	−0.022	0.174	−0.999*	0.868	0.984	−0.852
ko04662 B cell receptor signaling pathway	−0.460	−0.278	−0.882	0.560	0.805	−0.996*
ko04664 Fc epsilon RI signaling pathway	−0.809	−0.679	−0.578	0.130	0.454	−0.932
ko04666 Fc gamma R-mediated phagocytosis	−0.856	−0.940	0.528	−0.863	−0.645	−0.028
ko04670 Leukocyte transendothelial migration	−0.333	−0.510	0.947	−0.987	−0.983	0.612

Note: Na^+, Na^+ concentration; K^+, K^+ concentration; NKA, Na^+K^+-ATPase activity; SOD, SOD activity; CAT, CAT activity; MDA, the MDA contents. *$p < 0.05$ indicated significant correlation relationship between physiological parameters and KEGG pathways.

Acknowledgements

This work was supported by Guangzhou Science and Technology Project [No. 201803020017] and National Natural Science Foundation of China [No. 31902427].

Appendix A. Supplementary data

Supplementary data to this article can be found online at https://doi.org/10.1016/j.fsi.2020.02.028.

References

[1] M. Su, J. Zhou, Z. Duan, J. Zhang, Transcriptional analysis of renal dopamine-mediated Na^+ homeostasis response to environmental salinity stress in *Scatophagus argus*, BMC Genom. 20 (2019) 418, https://doi.org/10.1186/s12864-019-5795-x.

[2] G. Boeuf, P. Payan, How should salinity influence fish growth? Comp. Biochem. Physiol. C Toxicol. Pharmacol. 130 (4) (2001) 411–423, https://doi.org/10.1016/S1532-0456(01)00268-X.

[3] T.J. Bowden, Modulation of the immune system of fish by their environment, Fish Shellfish Immunol. 25 (4) (2008) 373–383, https://doi.org/10.1016/j.fsi.2008.03.017.

[4] L. Vargas-Chacoff, E. Saavedra, R. Oyarzún, E. Martínez-Montaño, J.P. Pontigo, A. Yáñez, I. Ruiz-Jarabo, J.M. Mancera, E. Ortiz, C. Bertrán, Effects on the metabolism, growth, digestive capacity and osmoregulation of juvenile of Sub-Antarctic Notothenioid fish *Eleginops maclovinus* acclimated at different salinities, Fish Physiol. Biochem. 41 (6) (2015) 1369–1381, https://doi.org/10.1007/s10695-015-0092-3.

[5] L. Tort, Stress and immune modulation in fish, Dev. Comp. Immunol. 35 (12) (2011) 1366–1375, https://doi.org/10.1016/j.dci.2011.07.002.

[6] Ü. Acar, V. Parrino, O.S. Kesbiç, G. Lo Paro, C. Saoca, F. Abbate, S. Yılmaz, F. Fazio, Effects of different levels of pomegranate seed oil on some blood parameters and disease resistance against *Yersinia Ruckeri* in Rainbow Trout, Front. Physiol. 9 (2018) 596, https://doi.org/10.3389/fphys.2018.00596.

[7] T. Cappello, M. Maisano, A. Giannetto, V. Parrino, A. Mauceri, S. Fasulo, Neurotoxicological effects on marine mussel *Mytilus galloprovincialis* caged at petrochemical contaminated areas (eastern Sicily, Italy): ^{1}H NMR and immunohistochemical assays, Comp. Biochem. Physiol. C Toxicol. Pharmacol. 169 (2015) 7–15, https://doi.org/10.1016/j.cbpc.2014.12.006.

[8] F. Fazio, C. Saoca, G. Costa, A. Zumbo, G. Piccione, V. Parrino, Flow cytometry and automatic blood cell analysis in striped bass *Morone saxatilis* (Walbaum, 1792): a new hematological approach, Aquaculture 513 (2019) 734398, https://doi.org/10.1016/j.aquaculture.2019.734398.

[9] V. Parrino, G. Costa, C. Cannavà, E. Fazio, M. Bonsignore, S. Concetta, G. Piccione, F. Fazio, Flow cytometry and micro-Raman spectroscopy: identification of hemocyte populations in the mussel *Mytilus galloprovincialis* (Bivalvia: mytilidae) from faro lake and tyrrhenian sea (sicily, Italy), Fish Shellfish Immunol. 87 (2019) 1–8, https://doi.org/10.1016/j.fsi.2018.12.067.

[10] V. Parrino, O.S. Kesbiç, Ü. Acar, F. Fazio, Hot pepper (*Capsicum* sp.) oil and its effects on growth performance and blood parameters in rainbow trout (*Oncorhynchus mykiss*), Nat. Prod. Res. (2019) 1–5, https://doi.org/10.1080/14786419.2018.1550769.

[11] V. Parrino, T. Cappello, G. Costa, C. Cannavà, M. Sanfilippo, F. Fazio, S. Fasulo, Comparative study of haematology of two teleost fish (*Mugil cephalus* and *Carassius auratus*) from different environments and feeding habits, Eur. Zool. J. 85 (1) (2018) 193–199, https://doi.org/10.1080/24750263.2018.1460694.

[12] S.C. Birrer, T.B.H. Reusch, O. Roth, Salinity change impairs pipefish immune defence, Fish Shellfish Immunol. 33 (6) (2012) 1238–1248, https://doi.org/10.1016/j.fsi.2012.08.028.

[13] A. Cuesta, R. Laiz-Carrión, M.P.M. del Río, J. Meseguer, J.M. Mancera, M.A. Esteban, Salinity influences the humoral immune parameters of gilthead seabream (*Sparus aurata* L.), Fish Shellfish Immunol. 18 (3) (2005) 255–261, https://doi.org/10.1016/j.fsi.2004.07.009.

[14] I.-F. Jiang, V. Bharath Kumar, D.-N. Lee, C.-F. Weng, Acute osmotic stress affects Tilapia (*Oreochromis mossambicus*) innate immune responses, Fish Shellfish Immunol. 25 (6) (2008) 841–846, https://doi.org/10.1016/j.fsi.2008.09.006.

[15] A.M. Marc, C. Quentel, A. Severe, P.Y. Le Bail, G. Boeuf, Changes in some endocrinological and non-specific immunological parameters during seawater exposure in the brown trout, J. Fish. Biol. 46 (6) (1995) 1065–1081, https://doi.org/10.1111/j.1095-8649.1995.tb01410.x.

[16] J.F. Taylor, M.P. Needham, B.P. North, A. Morgan, K. Thompson, H. Migaud, The influence of ploidy on saltwater adaptation, acute stress response and immune function following seawater transfer in non-smolting rainbow trout, Gen. Comp. Endocrinol. 152 (2–3) (2007) 314–325, https://doi.org/10.1016/j.ygcen.2007.02.029.

[17] M. Schmitz, J. Douxfils, S.N.M. Mandiki, C. Morana, S. Baekelandt, P. Kestemont, Chronic hyperosmotic stress interferes with immune homeostasis in striped catfish (*Pangasianodon hypophthalmus*, S.) and leads to excessive inflammatory response during bacterial infection, Fish Shellfish Immunol. 55 (2016) 550–558, https://doi.org/10.1016/j.fsi.2016.06.031.

[18] F.S. Abou-Seedo, S. Dadzie, K.A. Al-Kanaan, Sexuality, sex change and maturation patterns in the yellowfin seabream, *Acanthopagrus latus* (Teleostei: sparidae) (Houttuyn, 1782), J. Appl. Ichthyol. 19 (2) (2003) 65–73, https://doi.org/10.1046/j.1439-0426.2003.00355.x.

[19] T. Nakabo, Fishes of Japan: with Pictorial Keys to the Species, English edition, Tokai University Press, Kanagawa, 2002.

[20] J.H. Xia, K.F. Xia, S.G. Jiang, Characterization of 11 polymorphic microsatellite loci in the yellowfin seabream *Acanthopagrus latus*, Mol. Ecol. Notes 6 (2006) 484–486, https://doi.org/10.1111/j.1471-8286.2006.01282.x.

[21] J.H. Xia, J.H. Huang, J.B. Gong, S.G. Jiang, Significant population genetic structure of yellowfin seabream *Acanthopagrus latus* in China, J. Fish. Biol. 73 (8) (2008) 1979–1992, https://doi.org/10.1111/j.1095-8649.2008.02010.x.

[22] Y.H. Hu, Y.J. Liu, L.X. Tian, H.J. Yang, G.Y. Liang, W. Gao, Optimal dietary carbohydrate to lipid ratio for juvenile Yellowfin Seabream (*Sparus latus*), Aquacult. Nutr. 13 (4) (2007) 291–297, https://doi.org/10.1111/j.1365-2095.2007.00476.x.

[23] X.Y. Wu, Y.J. Liu, L.X. Tian, K.S. Mai, H.J. Yang, G.Y. Liang, Effects of raw corn starch levels on growth, feed utilization, plasma chemical indices and enzyme activities in juvenile yellowfin seabream *Sparus latus* Houttuyn, Aquacult. Res. 38 (12) (2007) 1330–1338, https://doi.org/10.1111/j.1365-2109.2007.01812.x.

[24] X.Y. Wu, Y.J. Liu, L.X. Tian, K.S. Mai, H.J. Yang, Utilization of different raw and pre-gelatinized starch sources by juvenile yellowfin seabream *Sparus latus*, Aquacult. Nutr. 13 (5) (2007) 389–396, https://doi.org/10.1111/j.1365-2095.2007.00489.x.

[25] A.A. Movahedinia, A. Savari, H. Morovvati, P. Koochanin, J.G. Marammazi, M. Nafisi, The effects of changes in salinity on gill mitochondria-rich cells of Juvenile Yellowfin Seabream, *Acanthopagrus latus*, J. Biol. Sci. 9 (7) (2009) 710–720, https://doi.org/10.3923/jbs.2009.710.720.

[26] R. Farshadian, A.P. Salati, S. Keyvanshokooh, H. Pasha-Zanoosi, Physiological responses of Yellowfin seabream (*Acanthopagrus latus*) to acute salinity challenge, Mar. Freshw. Behav. Physiol. 51 (5) (2018) 313–325, https://doi.org/10.1080/10236244.2019.1573638.

[27] J.H. Xia, P. Liu, F. Liu, G. Lin, F. Sun, R. Tu, G.H. Yue, Analysis of stress-responsive transcriptome in the intestine of Asian seabass (*Lates calcarifer*) using RNA-Seq, DNA Res. 20 (5) (2013) 449–460, https://doi.org/10.1093/dnares/dst022.

[28] A.M. Bolger, M. Lohse, B. Usadel, Trimmomatic: a flexible trimmer for Illumina sequence data, Bioinformatics 30 (15) (2014) 2114–2120, https://doi.org/10.1093/bioinformatics/btu170.

[29] M.G. Grabherr, B.J. Haas, M. Yassour, J.Z. Levin, D.A. Thompson, I. Amit, X. Adiconis, L. Fan, R. Raychowdhury, Q. Zeng, Z. Chen, E. Mauceli, N. Hacohen, A. Gnirke, N. Rhind, F. di Palma, B.W. Birren, C. Nusbaum, K. Lindblad-Toh, N. Friedman, A. Regev, Full-length transcriptome assembly from RNA-seq data without a reference genome, Nat. Biotechnol. 29 (7) (2011) 644–652, https://doi.org/10.1038/nbt.1883.

[30] W. Li, A. Godzik, Cd-hit: a fast program for clustering and comparing large sets of protein or nucleotide sequences, Bioinformatics 22 (13) (2006) 1658–1659, https://doi.org/10.1093/bioinformatics/btl158.

[31] R. Smith-Unna, C. Boursnell, R. Patro, J.M. Hibberd, S. Kelly, TransRate: reference-free quality assessment of *de novo* transcriptome assemblies, Genome Res. 26 (2016) 1134–1144, https://doi.org/10.1101/gr.196469.115.

[32] F.A. Simão, R.M. Waterhouse, P. Ioannidis, E.V. Kriventseva, E.M. Zdobnov, BUSCO: assessing genome assembly and annotation completeness with single-copy orthologs, Bioinformatics 31 (19) (2015) 3210–3212, https://doi.org/10.1093/bioinformatics/btv351.

[33] B. Li, C.N. Dewey, RSEM: accurate transcript quantification from RNA-Seq data with or without a reference genome, BMC Bioinf. 12 (2011) 323, https://doi.org/10.1186/1471-2105-12-323.

[34] M.I. Love, W. Huber, S. Anders, Moderated estimation of fold change and dispersion for RNA-seq data with DESeq2, Genome Biol. 15 (12) (2014) 550, https://doi.org/10.1186/s13059-014-0550-8.

[35] D.V. Klopfenstein, L. Zhang, B.S. Pedersen, F. Ramírez, A.W. Vesztrocy, A. Naldi, C.J. Mungall, J.M. Yunes, O. Botvinnik, M. Weigel, W. Dampier, C. Dessimoz, P. Flick, H. Tang, GOATOOLS: a Python library for Gene Ontology analyses, Sci. Rep. 8 (2018) 10872, https://doi.org/10.1038/s41598-018-28948-z.

[36] X. Mao, T. Cai, J.G. Olyarchuk, L. Wei, Automated genome annotation and pathway identification using the KEGG Orthology (KO) as a controlled vocabulary, Bioinformatics 21 (19) (2005) 3787–3793, https://doi.org/10.1093/bioinformatics/bti430.

[37] D. Rizopoulos, ltm: an R package for latent variable modelling and item response theory analyses, J. Stat. Software 17 (5) (2006) 1–25 http://www.jstatsoft.org/v17/i05/.

[38] J.D. Storey, A.J. Bass, A. Dabney, Robinson D. qvalue, Q-value estimation for false discovery rate control. R package version, 2.18.0, 2019. http://github.com/jdstorey/qvalue.

[39] D.H. Evans, Teleost fish osmoregulation: what have we learned since august krogh, homer smith, and ancel keys, Am. J. Physiol. Regul. Integr. Comp. Physiol. 295 (2) (2008) R704–R713, https://doi.org/10.1152/ajpregu.90337.2008.

[40] P. Laurent, S. Dunel, Morphology of gill epithelia in fish, Am. J. Physiol. Regul. Integr. Comp. Physiol. 238 (1980) R147–R159, https://doi.org/10.1152/ajpregu.1980.238.3.R147.

[41] L. Gui, P. Zhang, X. Liang, M. Su, D. Wu, J. Zhang, Adaptive responses to osmotic stress in kidney-derived cell lines from *Scatophagus argus*, a euryhaline fish, Gene 583 (2016) 134–140, https://doi.org/10.1016/j.gene.2016.02.026.

[42] R. Laiz-Carrion, P.M. Gurreiro, J. Fuentes, A.V.M. Canario, M.P. Martin Del Rio, J.M. Mancera, Branchial osmoregulatory response to salinity in the gilthead sea bream, *Sparus auratus*, J. Exp. Zool. 303A (7) (2005) 563–576, https://doi.org/10.1002/jez.a.183.

[43] R. Capela, J. Raimundo, M.M. Santos, M. Caetano, C. Micaelo, C. Vale, L. Guimarães, M.A. Reis-Henriques, The use of biomarkers as integrative tools for

transitional water bodies monitoring in the Water Framework Directive context - a holistic approach in Minho river transitional waters, Sci. Total Environ. 539 (2016) 85–96, https://doi.org/10.1016/j.scitotenv.2015.08.113.
[44] M. Zheng, J. Lu, D. Zhao, Effects of starch-coating of magnetite nanoparticles on cellular uptake, toxicity and gene expression profiles in adult zebrafish, Sci. Total Environ. 622–623 (2018) 930–941, https://doi.org/10.1016/j.scitotenv.2017.12.018.
[45] M. Zheng, J. Lu, G. Lin, H. Su, J. Sun, T. Luan, Dysbiosis of gut microbiota by dietary exposure of three graphene-family materials in zebrafish (*Danio rerio*), Environ. Pollut. 254 (2019) 112969, https://doi.org/10.1016/j.envpol.2019.112969.
[46] J.A. Adeyemi, Oxidative stress and antioxidant enzymes activities in the African catfish, *Clarias gariepinus*, experimentally challenged with *Escherichia coli* and *Vibrio fischeri*, Fish Physiol. Biochem. 40 (2014) 347–354, https://doi.org/10.1007/s10695-013-9847-x.
[47] M. Zheng, J. Lu, D. Zhao, Toxicity and transcriptome sequencing (RNA-seq) analyses of adult zebrafish in response to exposure carboxymethyl cellulose stabilized iron sulfide nanoparticles, Sci. Rep. 8 (2018) 8083, https://doi.org/10.1038/s41598-018-26499-x.
[48] A.L. Fernandes, J.P. Nascimento, A.P. Santos, C.A. Furtado, L.A. Romano, C.E. da Rosa, J.M. Monserrat, J. Ventura-Lima, Assessment of the effects of graphene exposure in *Danio rerio*: a molecular, biochemical and histological approach to investigating mechanisms of toxicity, Chemosphere (2018) 458–466, https://doi.org/10.1016/j.chemosphere.2018.06.183.
[49] D.G. McDonald, The effects of H^+ upon the gills of freshwater fish, Can. J. Zool. 61 (4) (1983) 691–703, https://doi.org/10.1139/z83-093.
[50] E. Fanta, F.S. Rios, S. Romao, A.C.C. Vianna, S. Freiberger, Histopathology of the fish *Corydoras paleatus* contaminated with sublethal levels of organophosphorus in water and food, Ecotoxicol. Environ. Saf. 54 (2003) 119–130, https://doi.org/10.1016/S0147-6513(02)00044-1.
[51] E.E. Deane, N.Y.S. Woo, Differential gene expression associated with euryhalinity in sea bream (*Sparus sarba*), Am. J. Physiol. Regul. Integr. Comp. Physiol. 287 (5) (2004) R1054–R1063, https://doi.org/10.1152/ajpregu.00347.2004.
[52] X. Zhang, H. Wen, H. Wang, Y. Ren, J. Zhao, Y. Li, RNA-Seq analysis of salinity stress-responsive transcriptome in the liver of spotted sea bass (*Lateolabrax maculatus*), PloS One 12 (3) (2017) e0173238, , https://doi.org/10.1371/journal.pone.0173238.
[53] D.A. Plouffe, P.C. Hanington, J.G. Walsh, E.C. Wilson, M. Belosevic, Comparison of select innate immune mechanisms of fish and mammals, Xenotransplantation 12 (4) (2005) 266–277, https://doi.org/10.1111/j.1399-3089.2005.00227.x.
[54] T. Wang, C.J. Secombes, Complete sequencing and expression of three complement components, C1r, C4 and C1 inhibitor, of the classical activation pathway of the complement system in rainbow trout *Oncorhynchus mykiss*, Immunogenetics 55 (9) (2003) 615–628, https://doi.org/10.1007/s00251-003-0622-5.
[55] J.H. Xia, G.H. Yue, Identification and analysis of immune-related transcriptome in Asian seabass *Lates calcarifer*, BMC Genom. 11 (2010) 356, https://doi.org/10.1186/1471-2164-11-356.
[56] M. Schmitz, T. Ziv, A. Admon, S. Baekelandt, S.N.M. Mandiki, M. L'Hoir, P. Kestemont, Salinity stress, enhancing basal and induced immune responses in striped catfish *Pangasianodon hypophthalmus* (Sauvage), Journal of Proteomics 167 (7) (2017) 21–24, https://doi.org/10.1016/j.jprot.2017.08.005.
[57] W.R. Heath, F.R. Carbone, Cross-presentation in viral immunity and self-tolerance, Nat. Rev. Immunol. 1 (2001) 126–134, https://doi.org/10.1038/35100512.
[58] P.E. Jensen, Recent advances in antigen processing and presentation, Nat. Immunol. 8 (10) (2007) 1041–1048, https://doi.org/10.1038/ni1516.
[59] G. Huang, Y. Wang, H. Chi, Regulation of TH17 cell differentiation by innate immune signals, Cell. Mol. Immunol. 9 (2012) 287–295, https://doi.org/10.1038/cmi.2012.10.
[60] T.R. Mosrnann, R.L. Coffman, TH1 and TH2 cells: different patterns of lymphokine secretion lead to different functional properties, Annu. Rev. Immunol. 7 (1989) 145–173, https://doi.org/10.1146/annurev.iy.07.040189.001045.